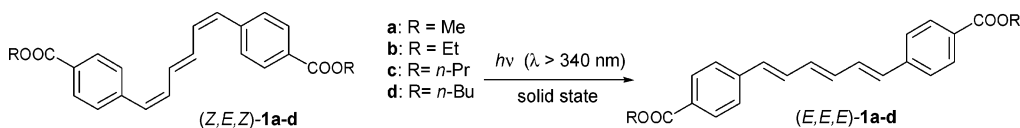# JOC Article

Crystalline-State *Z,E*-Photoisomerization of a Series of (*Z,E,Z*)-1,6-Diphenylhexa-1,3,5-triene 4,4′-Dicarboxylic Acid Dialkyl Esters. Chain Length Effects on the Crystal Structure and Photoreactivity[†]

Yoriko Sonoda,*,[‡] Yuji Kawanishi,[‡] Seiji Tsuzuki,[§] and Midori Goto[||]

Nanotechnology Research Institute and Technical Center, National Institute of Advanced Industrial Science and Technology (AIST), Higashi 1-1-1, Tsukuba, Ibaraki 305-8565, Japan, and Research Institute of Computational Sciences, National Institute of Advanced Industrial Science and Technology (AIST), Umezono 1-1, Tsukuba, Ibaraki 305-8568, Japan

y.sonoda@aist.go.jp

Crystalline-state *Z,E*-photoisomerization of a series of (*Z,E,Z*)-1,6-diphenylhexa-1,3,5-triene 4,4′-dicarboxylic acid dialkyl (R) esters [(*Z,E,Z*)-**1a**, R = Me; (*Z,E,Z*)-**1b**, R = Et; (*Z,E,Z*)-**1c**, R = *n*-Pr; (*Z,E,Z*)-**1d**, R = *n*-Bu] was investigated. All *Z,E,Z* isomers underwent one-way isomerization to the corresponding *E,E,E* isomers. The reaction efficiency was strongly enhanced as the length of the alkyl chain increased. Single-crystal X-ray analyses of (*Z,E,Z*)-**1a**−**d** showed that the alkyl chain part of the crystals became larger as the chain length increased. The conformational flexibility of the alkyl chains made the large change in the triene geometry in the lattice possible, leading to the enhancement of the photoreactivity in the crystalline state.

Introduction

Organic photoreactions in the solid state are attracting increased attention at the present time. The crystalline-state photopolymerization of diacetylenes[1] and diolefins[2] are well-known, and more recently, the polymerization of conjugated dienes has been reported.[3] For olefinic compounds in the crystalline state, one of the most common photoreactions would be [2+2] cycloaddition.[4,5] The *Z,E*-photoisomerization of olefins in restricted media has also received considerable attention;[6] however, the crystalline-state photoisomerization is relatively rare. The reaction has been reported for only a few kinds of compounds[7] such as (*Z*)-1,2-di(1-naphthyl)ethylene,[8,9] aromatic retinoids,[10] and (*Z,Z*)-muconates[11] up to now. It is obvious that the large changes in the molecular

---

[†] Y.S. dedicates this article to Prof. Michinori Ōki on the occasion of his 77th birthday.

* Author to whom correspondence should be addressed. Fax: +81-29-861-4673.

[‡] Nanotechnology Research Institute, National Institute of Advanced Industrial Science and Technology (AIST).

[§] Research Institute of Computational Sciences, National Institute of Advanced Industrial Science and Technology (AIST).

[||] Technical Center, National Institute of Advanced Industrial Science and Technology (AIST).

(1) Sarkar, A.; Okada, S.; Matsuzawa, H.; Matsuda, H.; Nakanishi, H. *J. Mater. Chem.* **2000**, *10*, 819.

(2) (a) Coates, G. W.; Dunn, A. R.; Henling, L. M.; Ziller, J. W.; Lobkovsky, E. B.; Grubbs, R. H. *J. Am. Chem. Soc.* **1998**, *120*, 3641. (b) Takahashi, S.; Miura, H.; Kasai, H.; Okada, S.; Oikawa, H.; Nakanishi, H. *J. Am. Chem. Soc.* **2002**, *124*, 10944.

(3) (a) Matsumoto, A.; Odani, T. *Macromol. Rapid Commun.* **2001**, *22*, 1195. (b) Matsumoto, A. *Polymer* J. **2003**, *35*, 93.

(4) (a) Ramamurthy, V.; Venkatesan, K. *Chem. Rev.* **1987**, *87*, 433. (b) Ito, Y. *Synthesis* **1998**, *1*, 1. (c) Sonoda, Y. In *CRC Handbook of Organic Photochemistry and Photobiology*, 2nd ed.; Horspool, W., Lenci, F., Eds.; CRC Press: Boca Raton, FL, 2004; Chapter 73.

(5) (a) Singh, A. K.; Krishina, T. S. R. *J. Phys. Chem. A.* **1997**, *101*, 3066. (b) Sonoda, Y.; Miyazawa, A.; Hayashi, S.; Sakuragi, M. *Chem. Lett.* **2001**, 410. (c) Gao, X.; Friščić, T.; MacGillivray, L. R. *Angew. Chem., Int. Ed.* **2004**, *43*, 232. (d) Caronna, T.; Liantonio, R.; Logothetis, T. A.; Metrangolo, P.; Pilati, T.; Resnati, G. *J. Am. Chem. Soc.* **2004**, *126*, 4500. (e) Papaefstathiou, G. S.; Zhong, Z.; Geng, L.; MacGillivray, L. R. *J. Am. Chem. Soc.* **2004**, *126*, 9158.

(6) (a) Liu, R. S. H. *Acc. Chem. Res.* **2001**, *34*, 555. (b) Liu, R. S. H.; Hammond, G. S. *Chem. Eur. J.* **2001**, *7*, 4536. (c) Liu, R. S. H. *Photochem. Photobiol*. **2002**, *76*, 580.

(7) (a) Scheffer, J. R.; Garcia-Garibay, M.; Nalamasu, O. In *Organic Photochemistry*; Padwa, A., Ed.; Marcel Dekker: New York, 1987; Vol. 8, Chapter 4. (b) Scheffer, J. R.; Pokkuluri, P. R. In *Photochemistry in Organized and Constrained Media*; Ramamurthy, V., Ed.; VCH: New York, 1991; Chapter 5.

(8) Alfimov, M. V.; Razumov, V. F. *Mol. Cryst. Liq. Cryst.* **1978**, *49* (Lett.), 95.

(9) Aldoshin, S. M.; Alfimov, M. V.; Atovmian, L. O.; Kaminsky, V. F.; Razumov, V. F.; Rachinsky, A. G. *Mol. Cryst. Liq. Cryst.* **1984**, *108*, 1.

(10) Pfoertner, K.-H.; Englert, G.; Schoenholzer, P. *Tetrahedron* **1987**, *43*, 1321.

geometry required by *Z,E*-photoisomerization are difficult to occur in the limited space of the rigid crystal lattice, since they usually accompany the large changes in molecular size and volume. This means that the easiness of the movements of the double-bond carbon atoms in the lattice plays a key role in determining the *Z,E*-photoisomerization reactivity in the crystalline state. It is therefore expected that, if an olefinic molecule has large conformational flexibility, it can easily isomerize in the crystal lattice without the large change in the total molecular size. The easiness of the atomic movements in the lattice is, of course, closely related to the crystal structure. However, our knowledge about the crystalline-state photoisomerization is highly fragmental. Because of lack of systematic study, the relationship between the crystal structure and the photoisomerization reactivity is not clear at present.

During our study on the *Z,E*-photoisomerization of various kinds of ring-substituted (*E,E,E*)-1,6-diphenyl-hexa-1,3,5-trienes [(*E,E,E*)-DPHs] in solution,[12] we have accidentally found that the dimethyl ester of (*Z,E,Z*)-DPH 4,4′-dicarboxylic acid, (*Z,E,Z*)-**1a**, underwent photoisomerization in the solid state. The ester derivatives of the acid having longer alkyl chains than methyl were expected to be easily obtained by Wittig reactions from corresponding alkyl 4-formylbenzoates. Since the easiness of the atomic movements of the triene carbons in the crystal should strongly be affected by the alkyl chain length, the investigation of the *Z,E*-photoisomerization behaviors and crystal structures for these esters would afford new insight into the structure−property relationship for the crystalline-state *Z,E*-isomerization. In this study, single crystals of a series of (*Z,E,Z*)-DPH 4,4′-dicarboxylic acid dialkyl esters, (*Z,E,Z*)-**1a-d** (Scheme 1), were prepared and their crystal structures and photoisomerization behaviors were systematically investigated.

Results and Discussion

1. Preparation of (*Z,E,Z*)-1a−d. Compounds (*Z,E,Z*)-**1a−d** were prepared by the Wittig reactions of aldehydes **2a−d** and bis-phosphonium salt **3** (Scheme 1). The reactions gave *Z−E* isomeric mixtures of **1a−d**, from which crude (*Z,E,Z*)-**1a−d** were isolated (Experimental section). Single crystals of (*Z,E,Z*)-**1a** suitable for X-ray analysis were obtained by recrystallization of the crude compound from acetonitrile, and the crystals of (*Z,E,Z*)-**1b−d** were grown from their acetonitrile solutions by slow evaporation at room temperature. The structures of (*Z,E,Z*)-**1a−d** were confirmed by NMR, IR, and UV−vis absorption spectroscopy. The *Z,E,Z* isomers of DPHs have been unknown compounds as far as we know. They are not photochemically produced from the *E,E,E* isomers in solution.[12] Compounds (*Z,E,Z*)-**1a−d** were stable in the solid state at least for a year in the dark at room temperature.

(11) Odani, T.; Matsumoto, A.; Sada, K.; Miyata, M. *J. Chem. Soc., Chem. Commun.* **2001**, 2004.

(12) (a) Sonoda, Y.; Suzuki, Y. *J. Chem. Soc., Perkin Trans. 2* **1996**, 401. (b) Sonoda, Y.; Suzuki, Y. *Chem. Lett.* **1996**, 659. (c) Sonoda, Y.; Morii, H.; Sakuragi, M.; Suzuki, Y. *Chem. Lett.* **1998**, 349. (d) Sonoda, Y.; Kawanishi, Y.; Sakuragi, M. *Chem. Lett.* **1999**, 587. (e) Sonoda, Y.; Kwok, W. M.; Petrasek, Z.; Ostler, R.; Matousek, P.; Towrie, M.; Parker, A. W.; Phillips, D. *J. Chem. Soc., Perkin Trans. 2* **2001**, 308. (f) Sonoda, Y.; Kawanishi, Y. *Chem. Lett.* **2003**, *32*, 978.

SCHEME 1. Preparation of (*Z,E,Z*)-1a−d by Wittig Reactions and One-Way *Z,E*-Photoisomerization of (*Z,E,Z*)-1a−d in the Crystalline State
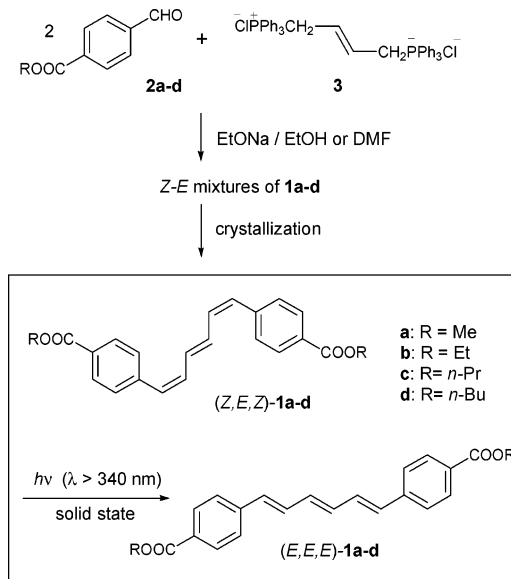
Although aldehydes **2a−d** had no ring substituent at the ortho positions to the formyl group, the products of the Wittig reactions were rich in *Z* isomers. It is known that the Wittig reactions of reactive aldehydes and phosphonium salts tend to give increased amount of *Z* isomers in the products.[13] In the present cases, the reactions were considerably fast because of the high reactivity of **2a−d** having electron-withdrawing alkyl ester groups. The enhanced reaction rates probably led to the favorable formation of (*Z,E,Z*)-**1a−d** by kinetic control.

2. Crystalline-State *Z,E*-Photoisomerization of (*Z,E,Z*)-1a-d. Irradiation of the single crystals of (*Z,E,Z*)-**1a−d** in air at room temperature induced *Z,E*-isomerization. The structures of the photoproducts were determined to be their *E,E,E* isomers from NMR, IR, and UV−vis spectra (Scheme 1). The photoreaction of (*Z,E,Z*)-**1a** was very clear. Compound (*E,E,E*)-**1a** was shown to be an exclusive product by HPLC. No [2+2] cycloaddition was observed. For (*Z,E,Z*)-**1b−d**, trace amounts of unknown compounds were detected in the photoproducts.

Figure 1 shows the solid-state UV−vis spectra before and after irradiation of (*Z,E,Z*)-**1a**. A weak and broad absorption was seen in the region of 340−450 nm before irradiation, whereas after irradiation, a strong and structured absorption was observed around 420 nm. It is clear that photoproduct (*E,E,E*)-**1a** absorbed the irradiation light of wavelength $\lambda > 340$ nm. However, the *E,E,E* isomer was photostable in the solid state. This led to *Z,E,Z→E,E,E* "one-way" isomerization.

The photoproducts from (*Z,E,Z*)-**1a−d** were analyzed by HPLC after various irradiation times. No *Z,E,E* isomer was found in the reaction mixtures even in the very early stages of the reactions. This shows that the reactions are not stepwise *Z,E,Z→Z,E,E→E,E,E* but concerted *Z,E,Z→E,E,E* isomerization, in which simultaneous *Z→E* isomerization occurs around the two *Z* double bonds in the *Z,E,Z* isomers. Irradiation of (*Z,E,Z*)-**1a** with light of

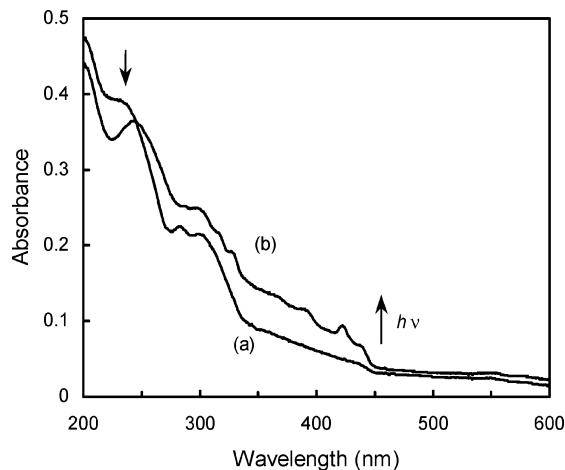(13) Maercker, A. *Org. React.* **1965**, *14*, 270.

FIGURE 1. UV–vis absorption spectra for the cast film of (*Z*,*E*,*Z*)-**1a** (a) before and (b) after irradiation. Irradiation time: 240 min.
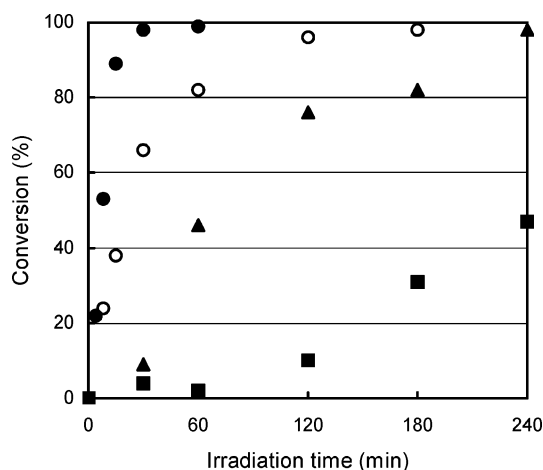

FIGURE 2. Time profile of the conversion for the photoisomerization of (*Z*,*E*,*Z*)-**1a–d** single crystals. (■) **1a**, (▲) **1b**, (○) **1c**, and (●) **1d**.

reduced intensity using a neutral density filter resulted in the considerable decrease in the rate of the reaction. Also in this case, however, no (*Z*,*E*,*E*)-**1a** was found in the reaction mixture.

When the crystals of (*Z*,*E*,*Z*)-**1a** were heated above its mp, thermal isomerization to (*E*,*E*,*E*)-**1a** occurred very slowly. When the crystals of (*Z*,*E*,*Z*)-**1b–d** were heated slightly above their mps, on the other hand, no amount or only a trace amount of the corresponding *E*,*E*,*E* isomers was detected. For (*E*,*E*,*E*)-**1a–d**, no thermal isomerization was observed even after heating above their mps.

Figure 2 shows the relationship between the irradiation time and the conversion for the reactions of (*Z*,*E*,*Z*)-**1a–d** single crystals. It is found that the reaction efficiency was strongly enhanced as the alkyl chain length increased.

Although the isomerization of (*Z*,*E*,*Z*)-**1a** was inefficient at its early stage, at the later stages, the reaction occurred more efficiently. The "introduction time" of 1–2 h was thus observed for the reaction. The conversion was lower than 50% even after being irradiated for 4 h or longer. This incompleteness of the photoreaction can be attributed to the fact that the pale yellow, transparent needles of (*Z*,*E*,*Z*)-**1a** became yellow powder on irradiation; the irradiation light did not reach the inner part of the crystals at the later stages of the reaction. The photoisomerization of (*Z*,*E*,*Z*)-**1a** occurred efficiently when its solution cast film was irradiated. No introduction time was seen for the film, and the reaction was completed after 4 h.

In contrast to the case of (*Z*,*E*,*Z*)-**1a**, the conversion reached 100% for (*Z*,*E*,*Z*)-**1b–d** (Figure 2). This corresponds to the fact that the (*Z*,*E*,*Z*)-**1b–d** crystals stayed almost transparent and therefore the irradiation light was able to reach the inner part of the crystals during the reactions. The introduction time for (*Z*,*E*,*Z*)-**1b** was ca. 0.5 h, which was considerably shorter than that for (*Z*,*E*,*Z*)-**1a**. No introduction time was observed for (*Z*,*E*,*Z*)-**1c** and (*Z*,*E*,*Z*)-**1d**.

3. Crystal Structures. Crystal Structures of (*Z*,*E*,*Z*)-1a–d. Table 1 shows the major structural parameters of (*Z*,*E*,*Z*)-**1a–d** obtained by X-ray crystal structure analyses. Their crystal data are summarized in Supporting Information Table S1.

Single-crystal X-ray analyses showed that molecules of (*Z*,*E*,*Z*)-**1a–d** were centrosymmetric. Figure 3 shows their ORTEP drawings. The structures of DPH moieties for (*Z*,*E*,*Z*)-**1a–d** were similar. The triene chains and aromatic rings were each planar for conjugation. The most characteristic features of the structures of these molecules are the twists around C3–C4 single bonds. The torsion angles (ϕ) of C2–C3–C4–C5 were ±40–$43°$ (Table 1). The twists around C3–C4 bonds largely contribute to the decrease in the steric hindrance between C1–H and C5–H hydrogens. The angles ϕ in (*Z*,*E*,*Z*)-**1a–d** are similar to the corresponding values in other (*Z*)-arylethylenes such as (*Z*)-1,2-di(1-naphthyl)ethylene ($\phi = 44.1°$)[9] and (*Z*)-dibenzo[*e*,*e*′]-3,3′-diazastilbene (39°).[14] Thus, the molecules of (*Z*,*E*,*Z*)-**1a–d** are twisted and bulky in the crystalline state, similar to other compounds showing the crystalline-state *Z*,*E*-photoisomerization.[7] The conformation of the methylene chains were all-trans in (*Z*,*E*,*Z*)-**1b–d**.

The structures of (*Z*,*E*,*Z*)-**1a** and (*Z*,*E*,*Z*)-**1d** were optimized by the HF/6-31G* level ab initio calculations. The calculated geometrical parameters including the torsion angles ϕ agree fairly well with those in crystals.

Figure 4 shows the projections from *c* axes for (*Z*,*E*,*Z*)-**1a–d**. In these crystals, the molecules were stacked parallel along *b* axes with π-conjugation planes. The packing patterns of the alkyl chains in (*Z*,*E*,*Z*)-**1a** and (*Z*,*E*,*Z*)-**1c** were different from those in (*Z*,*E*,*Z*)-**1b** and (*Z*,*E*,*Z*)-**1d**. The crystal systems of (*Z*,*E*,*Z*)-**1a** and (*Z*,*E*,*Z*)-**1c** were *P*2$_1$/*c*, whereas those of (*Z*,*E*,*Z*)-**1b** and (*Z*,*E*,*Z*)-**1d** were *C*2/*c* (Table S1). In Figure 4, two crystallographic repeating units were shown for (*Z*,*E*,*Z*)-**1a** and (*Z*,*E*,*Z*)-**1c** to compare with the cases of (*Z*,*E*,*Z*)-**1b** and (*Z*,*E*,*Z*)-**1d**. The lattice constant along the long molecular axis increased as the alkyl chain length increased; **1a**: $2a = 31.7$ Å, **1b**: $a = 35.3$ Å, **1c**: $2a = 39.3$ Å, and **1d**: $a = 44.9$ Å. The values of *b* and *c* were similar for all four compounds. Although the crystal systems of (*Z*,*E*,*Z*)-**1a**

(14) Vansant, J.; Smets, G.; Declercq, J. P.; Germain, G.; Van Meerssche, M. *J. Org. Chem.* **1980**, *45*, 1557.

TABLE 1. Major Structural Parameters[a] for (Z,E,Z)-1a–d Obtained from X-ray Crystal Structure Analyses

parameter	(Z,E,Z)-1a	(Z,E,Z)-1b	(Z,E,Z)-1c	(Z,E,Z)-1d
C1−C2	1.440(2)	1.445(3)	1.444(2)	1.447(3)
C3−C4	1.469(2)	1.472(2)	1.470(2)	1.473(3)
C1−C1^i	1.348(3)	1.358(3)	1.340(3)	1.351(4)
C2−C3	1.342(2)	1.344(3)	1.344(2)	1.349(3)
C4−C9	1.397(2)	1.399(2)	1.402(2)	1.404(2)
C4−C5	1.396(2)	1.395(2)	1.396(2)	1.402(2)
C5−C4−C9	117.8(1)	118.1(2)	117.8(1)	117.6(2)
C1^i−C1−C2	123.5(2)	123.1(2)	123.7(2)	123.5(2)
C1−C2−C3	128.4(1)	128.0(2)	128.3(1)	128.3(2)
C2−C3−C4	127.9(1)	127.8(2)	127.7(1)	128.0(2)
C1−C2−C3−C4	−1.5(2)	1.2(3)	1.3(2)	−1.3(3)
C2−C3−C4−C5	−41.0(2)	42.2(3)	42.6(2)	−40.8(2)
C1^i−C1−C2−C3	−179.9(2)	−179.9(2)	180.0(2)	179.8(2)
C6−C7−C10−O1	−0.2(2)	5.8(3)	6.8(2)	−4.9(3)
O1−C10−O2−C11	−1.8(2)	0.0(4)	1.2(2)	−2.3(3)
C7−C10−O2−C11	178.3(1)	178.0(2)	−179.5(1)	−179.2(2)
C10−O2−C11−C12		89.8(3)	91.8(2)	−104.6(2)
O2−C11−C12−C13			177.2(1)	−175.9(2)
C11−C12−C13−C14				172.0(3)

[a] In Å and degrees; for the numbering of atoms, see Figure 3. Symmetry codes: **1a**(i) −x, −y + 2, −z + 2; **1b** (i) −x + $^1/_2$, −y + $^1/_2$, −z + 2; **1c** (i)−x + 1, −y + 2, −z + 1; **1d** (i) −x + $^1/_2$, −y + $^1/_2$, −z + 2.
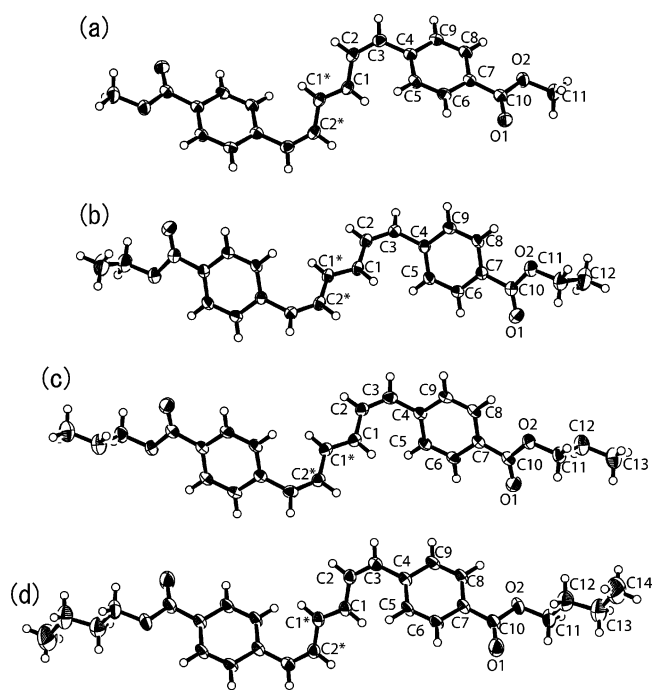

FIGURE 3. Views of the molecular structures of (Z,E,Z)-1a–d. (a) **1a**, (b) **1b**, (c) **1c**, and (d) **1d**. Displacement ellipsoids are drawn at the 50% probability level and H atoms are shown as small spheres of arbitrary radii. [Symmetry code: (*) −x+1, −y, −z+1.]

and (Z,E,Z)-**1c** were different from those of (Z,E,Z)-**1b** and (Z,E,Z)-**1d**, no even−odd effect was observed in their photoreactions.

The alkyl chain part of the crystals became larger as the chain lengths increased. For (Z,E,Z)-**1a**, a large part of the crystals was occupied by the π-stacked rigid conjugated triene and aromatic rings, whereas for (Z,E,Z)-**1d**, the flexible alkyl chains occupied a large part of the crystals. Values of mp and density decreased as the chain length increased, indicating that the strength of intermolecular interactions in the crystals decreased as the chain length increased (Table S1).

Powder X-ray Diffraction (XRD) Patterns before and after Irradiation. Figure 5a shows the powder XRD pattern of (Z,E,Z)-**1a** before irradiation. The pattern was in good agreement with the one calculated from the single-crystal data. On irradiation of (Z,E,Z)-**1a**, the intensity of the original peaks decreased and some new peaks appeared. The reaction was thus found to be crystal-to-crystal transformation. The positions of the new peaks of the photoproduced (E,E,E)-**1a** were identical to those for the "solution-grown" (E,E,E)-**1a** obtained by crystallization from toluene (see Experimental section) (Figure 5b). At present, however, the single-crystal X-ray analysis of neither the photoproduced nor the solution-grown (E,E,E)-**1a** is unsuccessful. Figure 5c shows the XRD pattern of the authentic (Z,E,E)-**1a**. The characteristic peak of (Z,E,E)-**1a** at 2θ = 7.62° was not observed during the isomerization, which is in accordance with the observation in the HPLC analysis.

Figure 6a shows the XRD pattern calculated from the single-crystal data of (Z,E,Z)-**1d** before irradiation. Figure 7 shows the pattern of (E,E,E)-**1d** measured after irradiation. For the photoproduced (E,E,E)-**1d**, the lattice constants of a and b were estimated from the figure to be 44 and 4.4 Å, respectively. Interestingly, they were near the values of a = 44.904(4) Å and b = 4.6750(4) Å for (Z,E,Z)-**1d** before irradiation. Figure 6b shows the calculated pattern based on the single-crystal data of the solution-grown (E,E,E)-**1d** obtained by recrystallization from toluene (see Experimental section). In contrast to the case of (E,E,E)-**1a**, the XRD pattern of the photoproduced (E,E,E)-**1d** was clearly different from that of its solution-grown crystals.

Crystal Structure of (E,E,E)-1d. Although the single-crystal X-ray analysis of the photoproduced (E,E,E)-**1d** was unsuccessful, the crystal data were able to be obtained for the solution-grown (E,E,E)-**1d**. Figures 8 and 9 show the ORTEP drawing and the packing diagram for the solution-grown (E,E,E)-**1d**, respectively. The crystal data and major structure parameters are listed in Table 2 and Supporting Information Table S2. The molecules were shown to be nearly planar, and the conformation of the methylene chains was all-trans.
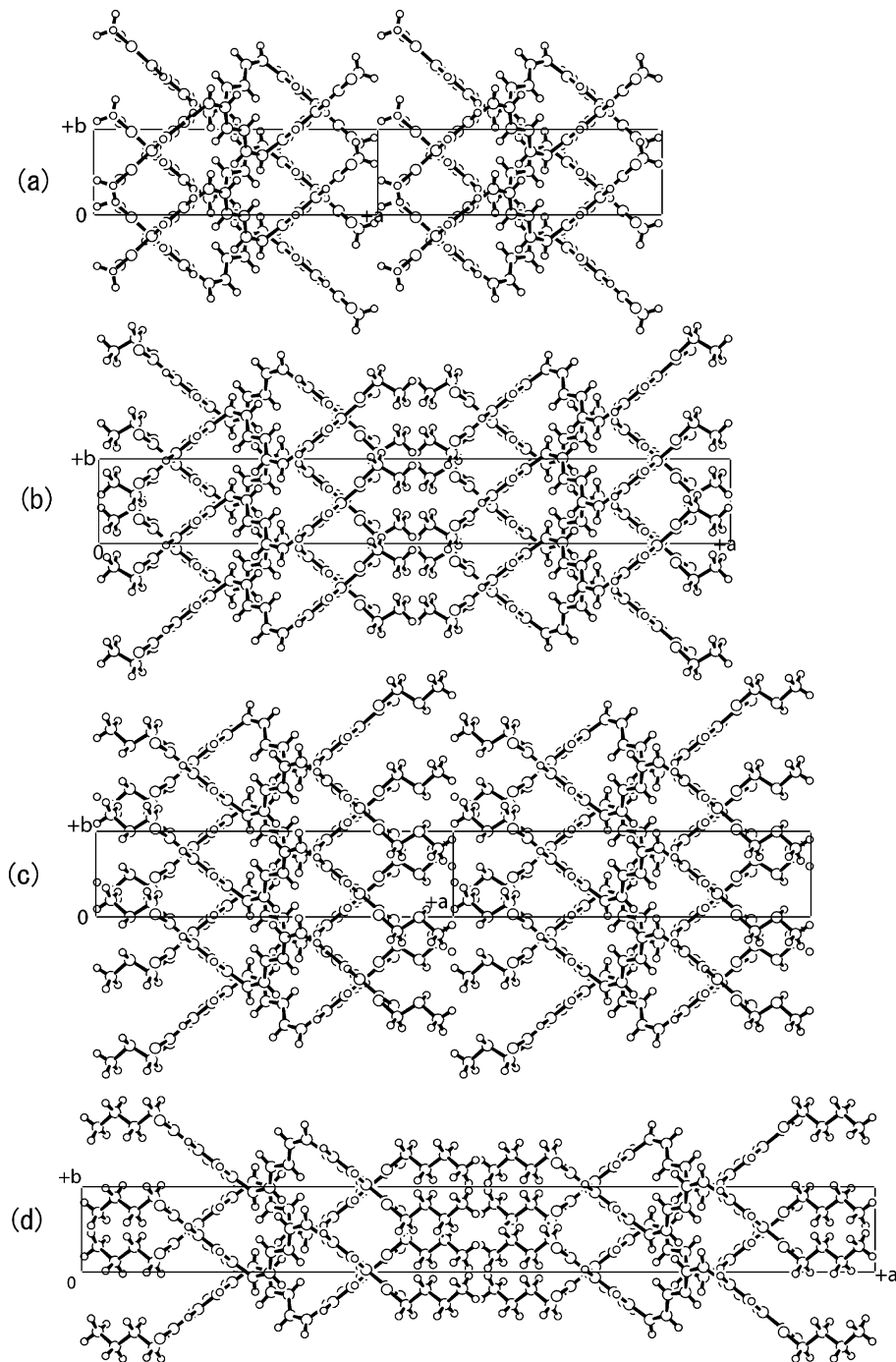
FIGURE 4. Packing diagrams for (*Z,E,Z*)-**1a**−**d** along the *c* axes. (a) **1a**, (b) **1b**, (c) **1c**, and (d) **1d**.

These structural features of the solution-grown (*E,E,E*)-**1d** are in good agreement with those predicted by ab initio calculation. The lattice constants for the solution-grown (*E,E,E*)-**1d** (Table S2) were very different from the value of *a* = 44 Å for the photoproduced (*E,E,E*)-**1d**. The crystal structure of the photoproduced (*E,E,E*)-**1d** was thus entirely different from that of the solution-grown (*E,E,E*)-**1d**.

4. Relationship between the Crystal Structure and the Photoisomerization Reactivity. Since the large part of the (*Z,E,Z*)-**1a** crystals was occupied by rigid conjugated double bonds and aromatic rings (Figure 4a), molecules were difficult to move in the lattice. As a result

of this, the photoreaction was inefficient at least at its earlier stage. However, once one of the (*Z,E,Z*)-**1a** molecules isomerized to (*E,E,E*)-**1a** in the lattice, the large change in molecular structure was expected to lead to the formation of structural defects in its neighborhood. The molecular motions became easier by such defects, and the reaction occurred more easily at its later stage. The enhanced photoreaction efficiency relative to that for the crystals and no introduction time for the cast film are easily understood by assuming that the crystal lattice of (*Z,E,Z*)-**1a** was partially destroyed before irradiation by dissolving the compound to prepare the solution cast film.
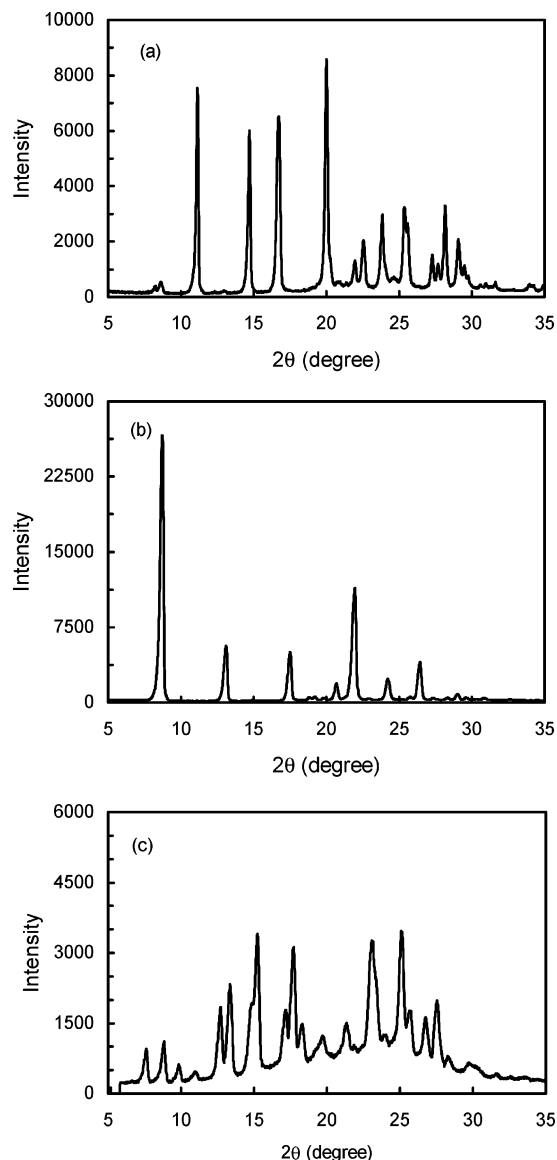
FIGURE 5. Powder XRD patterns of (a) *Z,E,Z*, (b) *E,E,E*, and (c) *Z,E,E* isomers of **1a**.

In the case of (*Z,E,Z*)-**1d**, the flexible *n*-butyl chains occupied a large part of the crystals (Figure 4d). The flexibility of the alkyl chains made the large change in the molecular geometry required by the isomerization possible, leading to the enhanced photoreactivity in the crystalline state. The fact that the lattice constant *a* = 44.904(4) Å for (*Z,E,Z*)-**1d** was near the value of *a* = 44 Å for the photoproduced (*E,E,E*)-**1d** suggests that the molecular length along the long axis did not change largely before and after the photoreaction. It is probable that the conformational changes in the alkyl chains play a key role in this case. The rigid DPH framework is expected to be nearly planar in the crystals of the photoproduced (*E,E,E*)-**1d** as well in those of the solution-grown (*E,E,E*)-**1d** (Figure 9). On the other hand, the methylene chains are flexible, and its conformation can at least partially be gauche in the photoproduced (*E,E,E*)-**1d**.

To evaluate the energy differences among various *n*-butyl conformers of (*E,E,E*)-**1d**, relative energies of
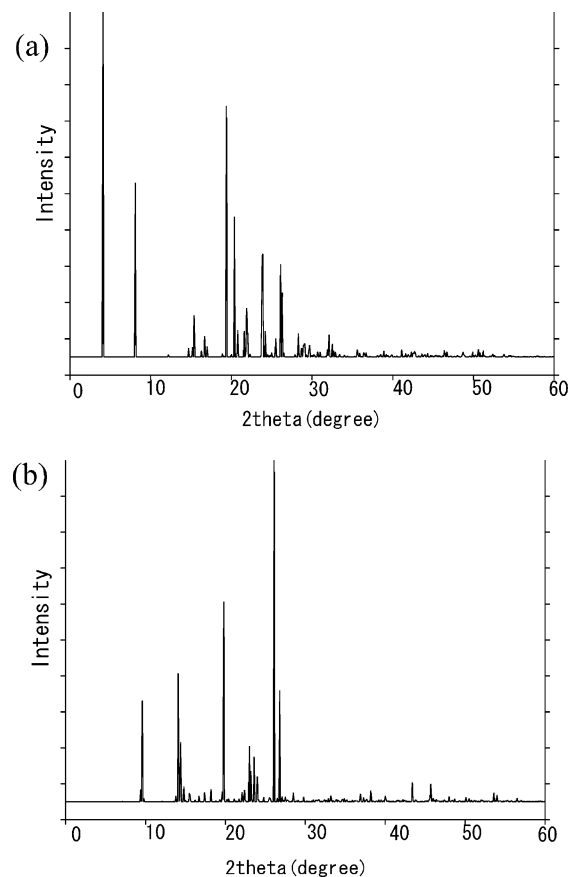

FIGURE 6. Powder XRD patterns calculated from single-crystal X-ray data. (a) (*Z,E,Z*)-**1d** before irradiation and (b) solution-grown (*E,E,E*)-**1d** obtained by recrystallization from toluene.
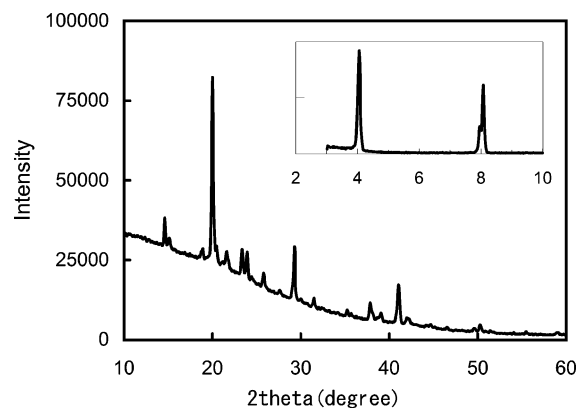

FIGURE 7. Powder XRD patterns measured after irradiation of (*Z,E,Z*)-**1d**.

conformers for *n*-butyl benzoic acid were calculated at the HF/6-311G* level. The calculations showed that some conformers having gauche bonds were only 1−2 kcal/mol less stable than the most stable all-trans conformer. It is very probable that the *n*-butyl chains in (*E,E,E*)-**1d** have some gauche bonds after the photoisomerization in the crystal, as the energy change associated with the conformational change of the *n*-butyl chains is not very large.

The molecular lengths along the long axes for (*Z,E,Z*)-**1d** and (*E,E,E*)-**1d** with all-trans butyl groups were
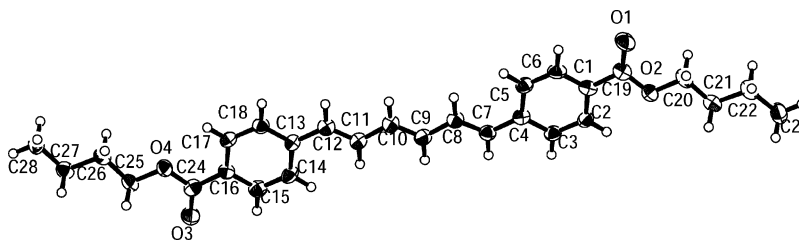
FIGURE 8. A view of the molecular structure of solution-grown (*E,E,E*)-**1d** obtained by recrystallization. Displacement ellipsoids are drawn at the 50% probability level and H atoms are shown as small spheres of arbitrary radii.
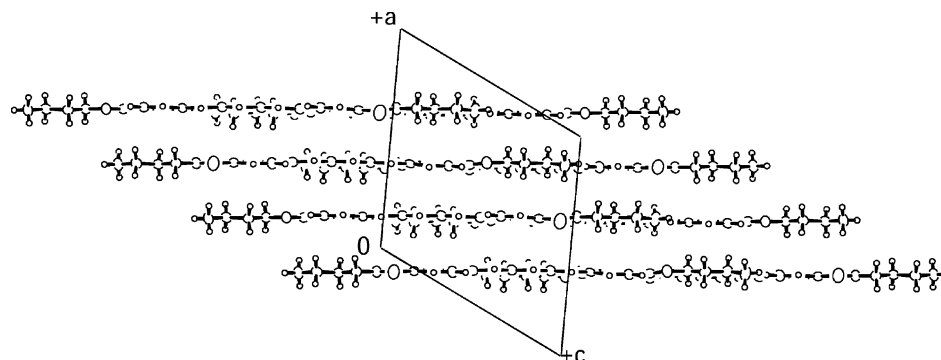

FIGURE 9. A packing diagram along the *b* axis for solution-grown (*E,E,E*)-**1d** obtained by recrystallization.

TABLE 2. Major Structural Parameters[a] for (*E,E,E*)-1d[b] Obtained from X-ray Crystal Structure Analysis

C8−C9	1.428(3)	C4−C7−C8−C9	−179.4(2)
C4−C7	1.459(3)	C5−C4−C7−C8	3.9(4)
C9−C10	1.339(3)	C7−C8−C9−C10	−177.3(2)
C7−C8	1.338(3)	C6−C1−C19−O1	−11.2(4)
C3−C4	1.397(3)	O1−C19−O2−C20	1.4(3)
C4−C5	1.402(3)	C1−C19−O2−C20	−178.2(2)
C3−C4−C5	117.7(2)	C19−O2−C20−C21	−171.7(2)
C8−C9−C10	124.9(2)	O2−C20−C21−C22	−179.9(2)
C7−C8−C9	123.8(2)	C20−C21−C22−C23	−177.1(2)
C4−C7−C8	126.7(2)		

[a] In Å and degrees; for the numbering of atoms, see Figure 8.
[b] Obtained by recrystallization from toluene.

FIGURE 10. One of the possible gauche conformers of (*E,E,E*)-**1d**; compare with its all-trans butyl conformer shown in Figure 8.

Experimental Section

Chemicals. Methyl 4-formylbenzoate (**2a**) was purchased and used without further purification. Ethyl, *n*-propyl, and *n*-butyl 4-formylbenzoates (**2b**, **2c**, and **2d**, respectively) were synthesized by similar procedures to that for *n*-octyl 4-formylbenzoate.[15] The purity of **2b**−**d** was checked by ^{1}H NMR spectra.[16,17] Bis-triphenylphosphonium salt **3** was prepared according to the literature.[18]

(*Z,E,Z*)-1,6-Diphenylhexa-1,3,5-triene 4,4′-Dicarboxylic Acid Dimethyl Ester [(*Z,E,Z*)-1a]. To a solution of methyl 4-formylbenzoate **2a** (1.50 g, 9.14 mmol) and salt **3** (2.97 g, 4.57 mmol) in ethanol (35 mL) was added a solution of sodium ethoxide in ethanol (0.30 M, 30 mL). The mixture was stirred under nitrogen atmosphere at room temperature. After stirring for 3 days, the resulting pale yellow precipitate was filtered off, washed with water (50 mL), and dried. The single crystals of (*Z,E,Z*)-**1a** were obtained by recrystallization of the crude product from acetonitrile. Yield 38%. Mp 172−173 °C; ^{1}H NMR (CDCl3) δ 8.03 (4H, d, *J* = 8.6 Hz, arom.), 7.41 (4H, d, *J* = 8.2 Hz, arom.), 6.87−6.99 (2H, m, triene 3-H and 4-H), 6.52 (2H, apparently (app.) d, *J* = 11.5 Hz, triene 1-H and 6-H), 6.32−

The increase in the molecular length that accompanied the triene *Z,E,Z→E,E,E* isomerization was predicted to be ca. 2.1 Å. On the other hand, the conformational analyses of *n*-butyl benzoic acid showed that the decrease in the molecular length that accompanied the trans→gauche conformational change in the butyl group was ca. 1 Å for one of the possible gauche conformers, whose energy was higher by only 1 kcal/mol than the all-trans conformer. It can therefore be expected that the trans→gauche changes in the two *n*-butyl groups of (*E,E,E*)-**1d** decrease the total molecular length of ca. 2 Å (Figure 10). Thus, the decrease in molecular length because of the butyl conformational changes can fully compensate for the increase in molecular length caused by the triene geometrical isomerization. Although s-trans→s-cis conformational changes in the triene can also lead to the decrease in the total molecular length of (*E,E,E*)-**1d**, the observed strong dependence of the photoreactivity on the chain length strongly suggests that the conformational changes in the alkyl groups are responsible for the highly efficient photoisomerization of (*Z,E,Z*)-**1d** in the limited space of the crystal lattice.
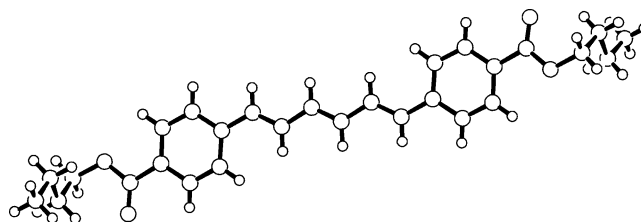
estimated from ab initio calculations to be 25.87 Å and 27.95 Å, respectively. Thus,

(15) Shao, X.-B.; Jiang, X.-K.; Wang, X.-Z.; Li, Z.-T.; Zhu, S.-Z. *Tetrahedron* **2003**, *59*, 4881.
(16) Konya, K. G.; Paul, T.; Lin, S.; Lusztyk, J.; Ingold, K. U. *J. Am. Chem. Soc.* **2000**, *122*, 7518.
(17) Lindsey, J. S.; Schreiman, I. C.; Hsu, H. C.; Kearney, P. C.; Marguerettaz, A. M. *J. Org. Chem.* **1987**, *52*, 827.
(18) McDonald, R. N.; Campbell, T. W. *J. Org. Chem.* **1959**, *24*, 1969.

6.48 (2H, m, triene 2-H and 5-H), 3.93 (6H, s, $-CH_3$); ^{13}C NMR (CDCl$_3$) δ 166.9 (C=O), 142.0 (arom. C-1), 132.1 (triene C-2 and C-5), 131.8 (triene C-3 and C-4), 130.2 (triene C-1 and C-6), 129.6 (arom. C-3 and C-5), 128.9 (arom. C-2 and C-6), 128.6 (arom. C-4), 52.1 (CH$_3$); IR (KBr) ν_{max} 1718, 1605, 1415, 1282, 1170, 1110, 1001, 950, 869, and 784 cm^{-1}; UV−vis (MeCN) λ_{max} (ϵ) 353 nm (41400); HR-MS calcd for C$_{22}$H$_{20}$O$_4$: 348.1361, found: 348.1375. Anal. calcd for C$_{22}$H$_{20}$O$_4$: C, 75.84; H, 5.79. Found: C, 76.01; H, 5.49.

(1Z,3E,5E)-1,6-Diphenylhexa-1,3,5-triene 4,4′-Dicarboxylic Acid Dimethyl Ester [(Z,E,E)-1a]. To the ethanol-soluble part of the crude product from **2a** and **3** was added water to give a 60% v/v aq ethanol solution. After this solution had been vigorously stirred, the resulting precipitate was filtered, washed with aq ethanol (60% v/v), and dried at room temperature. The Z,E,E isomer of **1a** was obtained as yellow solid. The purity was checked by HPLC. Yield 21%. Mp 87−89 °C; ^1H NMR (CDCl$_3$) δ 8.04 (2H, d, J = 8.2 Hz, arom.), 7.98 (2H, d, J = 8.6 Hz, arom.), 7.46 (2H, d, J = 8.6 Hz, arom.), 7.42 (2H, d, J = 8.2 Hz, arom.), 6.89−7.02 (2H, m, triene 3-H and 5-H), 6.65 (1H, d, J = 15.5 Hz, triene 6-H), 6.59−6.65 (1H, m, triene 4-H), 6.53 (1H, d, J = 12.2 Hz, triene 1-H), 6.43 (1H, app. t, J = 11.1 Hz, triene 2-H), 3.94 (3H, s, −CH$_3$), 3.91 (3H, s, −CH$_3$); ^{13}C NMR (CDCl$_3$) δ 166.9 and 166.8 (C=O), 142.1 and 141.6 (arom. C-1), 136.3, 132.6, 131.8, 131.4, 130.5, and 129.9 (triene), 130.0, 129.7, 128.9, and 126.3 (arom. C-2, C-3, C-5, and C-6), 129.0 and 128.6 (arom. C-4), 52.14 and 52.08 (CH$_3$); IR (KBr) ν_{max} 1714, 1602, 1434, 1279, 1177, 1106, 993, 960, 871, and 784 cm^{-1}; UV−vis (MeCN) λ_{max} (ϵ) 367 nm (55700); HR-MS calcd for C$_{22}$H$_{20}$O$_4$: 348.1361, found 348.1382. Compound (Z,E,E)-**1a** was somewhat unstable in air at room temperature; its UV−vis spectrum significantly changed after standing for 2−3 months in the dark.

(E,E,E)-1,6-Diphenylhexa-1,3,5-triene 4,4′-Dicarboxylic Acid Dimethyl Ester [(E,E,E)-1a]. A saturated solution of (Z,E,Z)-**1a** or (Z,E,E)-**1a** in toluene was irradiated with Pyrex-filtered light. The resulting solution-grown crystals of (E,E,E)-**1a** were collected and dried at room temperature. Mp 250−251 °C (lit.,[19] 256−259 °C); ^1H NMR (CDCl$_3$) δ 7.99 (4H, d, J = 8.6 Hz, arom.), 7.47 (4H, d, J = 8.2 Hz, arom.), 6.91−7.09 (2H, m, triene 2-H and 5-H), 6.66 (2H, app. d, J = 15.5 Hz, triene 1-H and 6-H), 6.53−6.65 (2H, m, triene 3-H and 4-H), 3.92 (6H, s, −CH$_3$); ^{13}C NMR (CDCl$_3$) δ 166.8 (C=O), 141.7 (arom. C-1), 134.6, 132.4, and 131.3 (triene), 130.0 and 126.3 (arom. C-2, C-3, C-5, and C-6), 128.9 (arom. C-4), 52.1 (CH$_3$); IR (KBr) ν_{max} 2921, 1720, 1602, 1282, 1178, 1108, 995, 878, 838, 765, and 699 cm^{-1}; UV−vis (MeCN) λ_{max} (ϵ) 376 nm (78600); HR-MS calcd for C$_{22}$H$_{20}$O$_4$: 348.1361, found 348.1391.

(Z,E,Z)-1,6-Diphenylhexa-1,3,5-triene 4,4′-Dicarboxylic Acid Diethyl Ester [(Z,E,Z)-1b]. To a solution of ethyl 4-formylbenzoate **2b** (1.00 g, 5.61 mmol) and **3** (1.82 g, 2.80 mmol) in ethanol (30 mL) was added a solution of sodium ethoxide in ethanol (0.30 M, 18.7 mL). The mixture was stirred under nitrogen atmosphere at room temperature. After stirring for 24 h, the resulting pale yellow precipitate was filtered off, washed with water (50 mL), and dried. The ethanol-insoluble yellow solid was shown from NMR spectra to be a 6:4 mixture of (Z,E,Z)-**1b** and (E,E,E)-**1b**. This solid was recrystallized from acetonitrile to give pure (E,E,E)-**1b**. The mother liquid mainly contained (Z,E,Z)-**1b**, from which the solvent acetonitrile evaporated very slowly at room temperature in dark to give the single crystals of (Z,E,Z)-**1b**. Yield 21%. Mp 140−142 °C; ^1H NMR (CDCl$_3$) δ 8.04 (4H, d, J = 8.2 Hz, arom.), 7.41 (4H, d, J = 8.2 Hz, arom.), 6.86−6.99 (2H, m, triene 3-H and 4-H), 6.52 (2H, app. d, J = 11.5 Hz, triene 1-H and 6-H), 6.31−6.47 (2H, m, triene 2-H and 5-H), 4.39 (4H, q, J = 7.0 Hz, −CH$_2$-), 1.41 (6H, t, J = 7.3 Hz, −CH$_3$); ^{13}C NMR (CDCl$_3$) δ 166.4 (C=O), 141.9 (arom. C-1), 132.1 (triene C-2 and C-5), 131.7 (triene C-3 and C-4), 130.2 (triene C-1 and C-6), 129.6 (arom.

C-3 and C-5), 129.0 (arom. C-4), 128.9 (arom. C-2 and C-6), 61.0 (CH$_2$), 14.3 (CH$_3$); IR (KBr) ν_{max} 2986, 1723, 1607, 1277, 1170, 1104, 1002, 950, 870, 792, and 738 cm^{-1}; UV−vis (MeCN) λ_{max} (ϵ) 352 nm (54100); HR-MS calcd for C$_{24}$H$_{24}$O$_4$: 376.1672, found 376.1630.

(E,E,E)-1,6-Diphenylhexa-1,3,5-triene 4,4′-Dicarboxylic Acid Diethyl Ester [(E,E,E)-1b]. Compound (E,E,E)-**1b** was obtained by recrystallization of the crude product from **2b** and **3**, as described above. Mp 184−186 °C; ^1H NMR (CDCl$_3$) δ 8.00 (4H, d, J = 8.2 Hz, arom.), 7.47 (4H, d, J = 8.2 Hz, arom.), 6.91−7.08 (2H, m, triene 2-H and 5-H), 6.65 (2H, app. d, J = 15.2 Hz, triene 1-H and 6-H), 6.54−6.65 (2H, m, triene 3-H and 4-H), 4.38 (4H, q, J = 7.1 Hz, −CH$_2$−), 1.40 (6H, t, J = 7.1 Hz, −CH$_3$); ^{13}C NMR (CDCl$_3$) δ 166.4 (C=O), 141.5 (arom. C-1), 134.6, 132.4, and 131.2 (triene), 130.0 and 126.2 (arom. C-2, C-3, C-5, and C-6), 129.3 (arom. C-4), 60.9 (CH$_2$), 14.3 (CH$_3$); IR (KBr) ν_{max} 2918, 1717, 1603, 1416, 1282, 1178, 1107, 997, 876, 837, 765, and 697 cm^{-1}; UV−vis (MeCN) λ_{max} (ϵ) 376 nm (81500); HR-MS calcd for C$_{24}$H$_{24}$O$_4$: 376.1672, found 376.1670.

(Z,E,Z)-1,6-Diphenylhexa-1,3,5-triene 4,4′-Dicarboxylic Acid Di(n-propyl) Ester [(Z,E,Z)-1c]. To a solution of n-propyl 4-formylbenzoate **2c** (1.00 g, 5.20 mmol) and **3** (1.76 g, 2.71 mmol) in ethanol (15 mL) was added a solution of sodium ethoxide in ethanol (0.30 M, 17.3 mL). The mixture was stirred under nitrogen atmosphere at room temperature. After stirring for 20 h, the resulting yellow precipitate was filtered off, washed with water (30 mL), and dried. The ethanol-insoluble yellow solid was shown to be a 1:1 mixture of (Z,E,Z)-**1c** and (E,E,E)-**1c** by NMR. The isomeric mixture was partially dissolved in a small portion of ethanol and was filtered. The ethanol filtrate was cooled to 0 °C (ice bath), and the resulting yellow solid ((Z,E,Z)-**1c**) was filtered off and dissolved in acetonitrile. Single crystals of (Z,E,Z)-**1c** were grown from this solution by very slow evaporation at room temperature in dark. Yield 15%. Mp 100−101 °C; ^1H NMR (CDCl$_3$) δ 8.04 (4H, d, J = 8.2 Hz, arom.), 7.41 (4H, d, J = 8.2 Hz, arom.), 6.87−6.99 (2H, m, triene 3-H and 4-H), 6.52 (2H, app. d, J = 11.2 Hz, triene 1-H and 6-H), 6.32−6.48 (2H, m, triene 2-H and 5-H), 4.30 (4H, t, J = 6.8 Hz, −OCH$_2$−), 1.75−1.88 (4H, m, −CH$_2$Me), 1.05 (6H, t, J = 7.4 Hz, −CH$_3$); ^{13}C NMR (CDCl$_3$) δ 166.4 (C=O), 141.9 (arom. C-1), 132.1 (triene C-2 and C-5), 131.7 (triene C-3 and C-4), 130.2 (triene C-1 and C-6), 129.6 (arom. C-3 and C-5), 129.0 (arom. C-4), 128.9 (arom. C-2 and C-6), 66.6 (OCH$_2$), 22.1 (CH$_2$Me), 10.5 (CH$_3$); IR (KBr) ν_{max} 2966, 1716, 1606, 1276, 1170, 1103, 1003, 950, 869, and 785 cm^{-1}; UV−vis (MeCN) λ_{max} (ϵ) 353 nm (58000); HR-MS calcd for C$_{26}$H$_{28}$O$_4$: 404.1986, found 404.2003.

(E,E,E)-1,6-Diphenylhexa-1,3,5-triene 4,4′-Dicarboxylic Acid Di(n-propyl) Ester [(E,E,E)-1c]. The isomeric mixture of (Z,E,Z)-**1c** and (E,E,E)-**1c** was irradiated in toluene with Pyrex-filtered light. The resulting crystals of (E,E,E)-**1c** were collected by filtration, recrystallized from toluene, and dried at room temperature. Mp 143−145 °C; ^1H NMR (CDCl$_3$) δ 8.00 (4H, d, J = 8.6 Hz, arom.), 7.47 (4H, d, J = 8.2 Hz, arom.), 6.90−7.08 (2H, m, triene 2-H and 5-H), 6.65 (2H, app. d, J = 15.5 Hz, triene 1-H and 6-H), 6.53−6.65 (2H, m, triene 3-H and 4-H), 4.28 (4H, t, J = 6.6 Hz, −OCH$_2$−), 1.73−1.87 (4H, m, −CH$_2$Me), 1.04 (6H, t, J = 7.4 Hz, −CH$_3$); ^{13}C NMR (CDCl$_3$) δ 166.4 (C=O), 141.5 (arom. C-1), 134.6, 132.4, and 131.2 (triene), 130.0 and 126.2 (arom. C-2, C-3, C-5, and C-6), 129.3 (arom. C-4), 66.5 (OCH$_2$), 22.1 (CH$_2$Me), 10.5 (CH$_3$); IR (KBr) ν_{max} 2974, 1714, 1602, 1415, 1280, 1177, 1109, 1000, 877, 837, 767, 698 cm^{-1}; UV−vis (MeCN) λ_{max} (ϵ) 377 nm (94600); HR-MS calcd for C$_{26}$H$_{28}$O$_4$: 404.1986, found 404.2006.

(Z,E,Z)-1,6-Diphenylhexa-1,3,5-triene 4,4′-Dicarboxylic Acid Di(n-butyl) Ester [(Z,E,Z)-1d]. To a solution of n-butyl 4-formylbenzoate **2d** (2.00 g, 9.70 mmol) and **3** (4.50 g, 6.93 mmol) in DMF (60 mL) was added a solution of sodium ethoxide in ethanol (0.60 M, 23 mL). The mixture was stirred under nitrogen atmosphere at room temperature. After stirring for 24 h, water (60 mL) was added to the reaction mixture,

(19) Mitsudo, T.; Fischetti, W.; Heck, R. F. *J. Org. Chem.* **1984**, *49*, 1640.

and the resulting pale yellow precipitate was filtered off. The precipitate was washed with aq ethanol (60−70% v/v, 600 mL) to remove any triphenylphosphine oxide and was dried at room temperature. The crude product was shown by NMR to be a 2:1 mixture of (*Z,E,Z*)-**1d** and (*E,E,E*)-**1d**. The isomeric mixture was partially dissolved in a small portion of acetonitrile. Single crystals of (*Z,E,Z*)-**1d** were grown from this acetonitrile solution by very slow evaporation of the solvent at room temperature in dark. Yield 7%. Mp 96−97 °C; ^{1}H NMR (CDCl$_3$) δ 8.03 (4H, d, *J* = 8.2 Hz, arom.), 7.41 (4H, d, *J* = 8.2 Hz, arom.), 6.87−6.99 (2H, m, triene 3-H and 4-H), 6.52 (2H, app. d, *J* = 11.5 Hz, triene 1-H and 6-H), 6.33−6.47 (2H, m, triene 2-H and 5-H), 4.34 (4H, t, *J* = 6.6 Hz, −OCH$_2$-), 1.72−1.82 (4H, m, −CH$_2$Et), 1.45−1.60 (4H, m, −CH$_2$Me), 0.99 (6H, t, *J* = 7.4 Hz, −CH$_3$); ^{13}C NMR (CDCl$_3$) δ 166.4 (C=O), 141.9 (arom., C-1), 132.1 (triene C-2 and C-5), 131.7 (triene C-3 and C-4), 130.2 (triene C-1 and C-6), 129.6 (arom. C-3 and C-5), 129.0 (arom. C-4), 128.9 (arom. C-2 and C-6), 64.9 (OCH$_2$), 30.8 (CH$_2$Et), 19.3 (CH$_2$Me), 13.8 (CH$_3$); IR (KBr) ν_{max} 2960, 1722, 1607, 1281, 1171, 1104, 1003, 950, 869, 783, and 729 cm^{-1}; UV−vis (MeCN) λ_{max} (ϵ) 351 nm (63600); HR-MS calcd for C$_{28}$H$_{32}$O$_4$: 432.2299, found 432.2352.

(*E,E,E*)-1,6-Diphenylhexa-1,3,5-triene 4,4′-Dicarboxylic Acid Di(*n*-butyl) Ester [(*E,E,E*)-1d]. A saturated solution of an isomeric mixture of (*Z,E,Z*)-**1d** and (*E,E,E*)-**1d** in toluene was irradiated with Pyrex-filtered light. The resulting solution-grown crystals (predominantly *E,E,E*) were collected and dried at room temperature. Recrystallization from toluene gave pure (*E,E,E*)-**1d**. Mp 133−134 °C; ^{1}H NMR (CDCl$_3$) δ 7.99 (4H, d, *J* = 8.2 Hz, arom.), 7.47 (4H, d, *J* = 8.2 Hz, arom.), 6.91−7.08 (2H, m, triene 2-H and 5-H), 6.65 (2H, app. d, *J* = 15.5 Hz, triene 1-H and 6-H), 6.53−6.65 (2H, m, triene 3-H and 4-H), 4.32 (4H, t, *J* = 6.6 Hz, −OCH$_2$−), 1.71−1.81 (4H, m, −CH$_2$Et), 1.42−1.56 (4H, m, −CH$_2$Me), 0.99 (6H, t, *J* = 7.3 Hz, −CH$_3$); ^{13}C NMR (CDCl$_3$) δ 166.4 (C=O), 141.5 (arom. C-1), 134.6, 132.4, and 131.2 (triene), 130.0 and 126.2 (arom. C-2, C-3, C-5, and C-6), 129.3 (arom. C-4), 64.8 (OCH$_2$), 30.8 (CH$_2$Et), 19.3 (CH$_2$Me), 13.8 (CH$_3$); IR (KBr) ν_{max} 2961, 1712, 1600, 1417, 1283, 1176, 1111, 998, 879, 833, 767, and 697 cm^{-1}; UV−vis (MeCN) λ_{max} (ϵ) 377 nm (103000); HR-MS calcd for C$_{28}$H$_{32}$O$_4$: 432.2299, found 432.2319.

Irradiation Experiments and Photoproduct Analyses. Irradiation experiments were carried out using a high-pressure mercury lamp (500 W) as a light source. The light was filtered with glass filters (λ > 340 nm). The irradiation was interrupted every 50−60 min by standing in the dark for 10 min to prevent any thermal reaction. The single crystals of (*Z,E,Z*)-**1a**−**d** were placed between quartz plates (10 × 40 mm^2) and were irradiated. The film sample of (*Z,E,Z*)-**1a** was prepared by casting its concentrated solution in dichloromethane on a quartz plate in the dark and by drying at room temperature in air. The irradiated samples were dissolved in acetonitrile in the dark and were submitted to HPLC analysis.

The photoproducts were analyzed using an HPLC monitored by a multichannel photodetector. The eluent was acetonitrile. The isomer ratio in the reaction mixture was determined from the ratio of HPLC peak area and the extinction coefficients of the *Z,E,Z* and *E,E,E* isomers of **1a**−**d** at the monitor wavelength. It was confirmed by NMR that the HPLC peak area

was proportional to the product of the isomer content and the extinction coefficient at monitor wavelengths.

Single-Crystal X-ray Structure Analyses. The single-crystal XRD measurements of the *Z,E,Z* isomers of **1a**−**d** and recrystallized (*E,E,E*)-**1d** were performed at 183 K using a CCD area-detector diffractometer with graphite monochromated MoKα radiation (λ = 0.71073 Å). Data collection, reduction, and empirical absorption correction were carried out using SMART, SAINTPLUS, and SADABS.[20] The structure was solved by direct methods using SIR92[21] and was refined by full matrix least squares on F^2 with SHELXTL.[22] The non-hydrogen atoms were refined anisotropically. Hydrogen atoms were placed in geometrically calculated positions and were refined by a riding model.

Powder XRD Pattern Measurements. The powder X-ray analysis data of (*Z,E,Z*)-**1a**, (*Z,E,E*)-**1a**, (*E,E,E*)-**1a**, and the photoproduced (*E,E,E*)-**1d** were obtained with a diffractometer with graphite monochromated Cu Kα radiation.

Computational Method. The Gaussian 98[23] program was used for the ab initio molecular orbital calculations. The 6-31G*, 6-311G** basis sets were used for the calculations.

Supporting Information Available: Crystallographic data for (*Z,E,Z*)-**1a**−**d** and (*E,E,E*)-**1d** in CIF format; general experimental information; analytical and spectroscopic data for **2b**−**d**; ^{1}H NMR spectra of (*Z,E,Z*)-**1a**−**d**, (*Z,E,E*)-**1a**, and (*E,E,E*)-**1a**−**d**; crystal and structure refinement data for (*Z,E,Z*)-**1a**−**d** and (*E,E,E*)-**1d**; results of the ab initio calculation for (*Z,E,Z*)-**1d** and (*E,E,E*)-**1d**, and the conformational analysis of *n*-butyl benzoate. This material is available free of charge via the Internet at http://pubs.acs.org.

JO051137G

(20) *SMART*, version 5.625; Bruker AXS: Madison, WI, 2001. *SAINTPLUS*, version 6.22; Bruker AXS: Madison, WI, 2001; Sheldrick, G. M. *SADABS*; Program for scaling and correction of area, detector data; University of Göttingen: Göttingen, Germany, 1998.

(21) Altomare, A.; Cascarano, G.; Giacovazzo, C.; Guagliardi, A.; Brula, M. C.; Polidori, G.; Camalli, M. *J. Appl. Crystallogr.* **1994**, *27*, 435.

(22) Sheldrick, G. M. *SHELXTL*, version 6.12; Bruker AXS: Madison, WI, 2000.

(23) Frisch, M. J.; Trucks, G. W.; Schlegel, H. B.; Scuseria, G. E.; Robb, M. A.; Cheeseman, J. R.; Zakrzewski, V. G.; Montgomery, J. A., Jr.; Stratmann, R. E.; Burant, J. C.; Dapprich, S.; Millam, J. M.; Daniels, A. D.; Kudin, K. N.; Strain, M. C.; Farkas, O.; Tomasi, J.; Barone, V.; Cossi, M.; Cammi, R.; Mennucci, B.; Pomelli, C.; Adamo, C.; Clifford, S.; Ochterski, J.; Petersson, G. A.; Ayala, P. Y.; Cui, Q.; Morokuma, K.; Malick, D. K.; Rabuck, A. D.; Raghavachari, K.; Foresman, J. B.; Cioslowski, J.; Ortiz, J. V.; Stefanov, B. B.; Liu, G.; Liashenko, A.; Piskorz, P.; Komaromi, I.; Gomperts, R.; Martin, R. L.; Fox, D. J.; Keith, T.; Al-Laham, M. A.; Peng, C. Y.; Nanayakkara, A.; Gonzalez, C.; Challacombe, M.; Gill, P. M. W.; Johnson, B. G.; Chen, W.; Wong, M. W.; Andres, J. L.; Head-Gordon, M.; Replogle, E. S.; Pople, J. A. *Gaussian 98*, revision A. 11; Gaussian, Inc.: Pittsburgh, PA, 1998.